



University of Zagreb  
Faculty of Mechanical  
Engineering and Naval  
Architecture

journal homepage: [www.brodogradnja.fsb.hr](http://www.brodogradnja.fsb.hr)

## Brodogradnja

An International Journal of Naval Architecture and  
Ocean Engineering for Research and Development



Optimization of marine propeller characteristics for maximum open water efficiency using an ANN-GA tool trained on experimental data



Carlo Giorgio Grlj<sup>1,\*</sup>, Nastia Degiuli<sup>1</sup>, Ivana Martić<sup>1</sup>, Marta Pedišić Buča<sup>2</sup>

<sup>1</sup>University of Zagreb, Faculty of Mechanical Engineering and Naval Architecture, Ivana Lučića 5, Zagreb 10000, Croatia

<sup>2</sup>Jadranbrod d.d., Avenija Većeslava Holjevca 20, Zagreb, 10000, Croatia

### ARTICLE INFO

Keywords:

Preliminary propeller design

Open water characteristics

Artificial Neural Network

Surrogate model

Bayesian regularization

Optimization

Genetic algorithm

### ABSTRACT

This study proposes a numerical approach for identifying the propeller characteristics that achieve maximum open water efficiency for a specific ship, considering its propulsion characteristics and defined operating conditions. The proposed method combines an artificial neural network (ANN) with an optimization procedure based on the genetic algorithm. The ANN is trained using experimentally obtained open water characteristics of 143 propellers, enabling accurate prediction of thrust and torque coefficients as well as the open water efficiency as functions of propeller geometric parameters. The optimal ANN achieved an  $R^2$  of 0.95 and  $RMSE$  of 0.20 on the validation set. Once trained, the ANN is integrated into the optimization procedure to explore the design space and identify the optimal propeller, while satisfying the imposed constraints. The approach is validated on several benchmark ships. The obtained results show good agreement with those from literature, despite the relatively small training dataset used in the present work. The obtained open water efficiencies are higher than those of the original propellers for all ships considered. It is demonstrated that the required propulsion characteristics used as input parameters can be obtained from different sources, including numerical simulations, experimental data, and empirical prediction methods such as the approach proposed by Holtrop and Mennen. For practical implementation, a standalone application was developed in MATLAB, integrating the trained ANN and genetic algorithm (GA) optimization procedure into a user-friendly environment.

### 1. Introduction

In ship design, the hydrodynamic performance of the propeller has a critical role in the determination of the ship overall efficiency, fuel consumption and, consequently, the environmental impact. Conventionally, propeller design can be carried out using systematic series data or regression formulae [1]. From the propeller main particulars: the pitch ratio  $P/D$ , expanded area ratio  $A_E/A_0$ , blade number  $Z$ , the corresponding open water characteristics are derived from systematic propeller series such as Wageningen B [2], Gawn [1], or Kaplan series. The final selection of the propeller is typically based on maximising open water efficiency  $\eta_o$

\* Corresponding author.

E-mail address: [carlo.g.grlj@fsb.unizg.hr](mailto:carlo.g.grlj@fsb.unizg.hr)

while satisfying the imposed constraints. This method relies on the open water curves derived from the towing tank tests for the different propeller series. Also, the optimal propellers from different series cannot be directly compared, as each design is optimized within the constraints of its respective series [3].

Recent advances in data-driven modelling have enabled more flexible and efficient alternatives. Artificial Neural Networks (ANN), owing to their capability to approximate highly nonlinear relationships, have been increasingly applied in ship design. In particular, ANNs have been used as surrogate models to predict ship resistance and propulsion characteristics, thereby significantly accelerating iterative design. Martić et al. [4] developed an ANN to predict the added resistance coefficient of containerships in regular head waves at various speeds. The data used for training the ANN is derived using boundary integral element method for various hull forms of containerships. This study enables a reliable prediction of added resistance coefficient during the preliminary ship design based on its characteristics and design speed. Ao et al. [5] developed a neural network using the results obtained with a low-fidelity method and with Computational Fluid Dynamics (CFD) simulations to predict the ship total resistance. The authors demonstrated that neural networks can be used to accurately predict the ship hydrodynamic performance. Lee and Lee [6] employed ANN with the intent to replace CFD simulations for the determination of wake distribution and total resistance. The proposed ANN was used in a multi-objective optimization procedure to enhance the wake distribution as well as to reduce the total resistance of a 1000 TEU containership. Degiuli et al. [7] employed different machine learning (ML) methods to develop models for the prediction of wind loads on containerships. The data for training the ML models are derived from CFD simulations for containership loaded with different container configurations at wind angles of attack from  $0^\circ$  to  $180^\circ$  performed by Grlj et al. [8]. More recently, Physics-Informed Neural Networks (PINNs) have been increasingly applied to a range of problems in ship hydrodynamics [9]. Tong and Chen [10] proposed a type of PINN trained on large eddy simulation data for the prediction of propeller wake and showed that a reconstruction of velocity and pressure fields can be obtained with minimal computational demand. Burchas and Papalambrou [11] developed a PINN for the prediction of ship main engine power with the given loading conditions and sea states. Their results demonstrate that the proposed PINN effectively captures the underlying physical principles, in contrast to conventional ML methods.

The integration of ANN-based surrogate models with optimization algorithms provides a powerful framework for improving ship energy efficiency. Hadavi et al. [12] developed an ANN and coupled it with Genetic Algorithm (GA) to identify optimal designs of ship masts with the aim to minimize the aerodynamic load on the ship. Lefkiou et al. [13] proposed a multitask deep neural network for the prediction of shear and pressure distributions on various Wigley-based hull forms. The trained neural network was incorporated into a GA optimization procedure to obtain an improved hull form that exhibited a 15.77 % reduction in total resistance compared to the baseline geometry. Optimization algorithms can be employed to lower the ship total resistance or improve propulsive efficiency by altering the ship hull or propeller geometry. Cheng et al. [14] generated fully parametric models of a ship, propeller, and rudder for an optimization study with the aim to lower the total resistance. The authors used CFD simulations to obtain the input data needed for the optimization study. An approximately 5 % reduction in delivered power was obtained with respect to the baseline geometry. Liu et al. [15] developed an ANN with numerical results as the training dataset for the prediction of hydrodynamic performance of an Autonomous and Remotely-operated Vehicle (ARV). The trained ANN was used to optimize the ARV geometry with the aim to minimise the dimensionless forces acting on it. Guo et al. [16] performed an optimization of the Korean Research Institute of Ships and Ocean Engineering (KRISO) containership (KCS) hull with the aim to minimise the total resistance by adjusting the bulbous bow. The authors employed Particle Swarm Optimization (PSO) algorithm for the optimization process and CFD simulations for obtaining the hydrodynamic loads acting on the ship. Zhao et al. [17] employed PSO within a numerical framework for selecting the optimal hull, propeller and main engine configuration, showing its potential in the ship design cycle.

In light of recent advancements in data-driven approaches to ship design, several studies have demonstrated the successful application of similar methodologies to preliminary propeller design. Vázquez-Santos et al. [18] employed the Non-dominated Sorting Genetic Algorithm-II (NSGA-II) to optimize the

Wageningen B-series propellers by maximising  $\eta_o$ , while minimising the engine brake power with constraints imposed for thrust and cavitation. The authors investigated the open water characteristics of the obtained propeller by conducting CFD simulations, which were validated against experimental data. Lu et al. [19] performed a multi-objective energy efficiency optimization for ships sailing in realistic conditions. Within the study, the authors optimized the propeller parameters with the objective of increasing propulsion efficiency, while decreasing the specific fuel oil consumption and nitrogen oxides emissions. Vesting and Bensow [20] proposed an optimization method based on PSO algorithm for propeller design. The authors found that the PSO algorithm yields comparable results to NSGA-II but with faster convergence and better solutions regarding constraint violations. Ouyang et al. [21] employed the NSGA-II for multi-objective optimization of rim-driven thrusters which resulted in a 5.78 % improvement of the maximal hydrodynamic efficiency. Zuo et al. [22] developed a Bayesian-optimized back-propagation neural network and employed the NSGA-III algorithm to obtain the optimal propeller design by simultaneously maximizing  $\eta_o$  and  $K_T$  while minimizing  $K_Q$ . Tadros et al. [3] developed an ANN that uses dimensionless propeller parameters as inputs to predict the corresponding open water characteristics. The trained model was subsequently employed to identify optimal propellers for selected ships across different propeller series. For the training dataset, the authors used the available thrust coefficients  $K_T$  and torque coefficients  $K_Q$  for propellers from different series. The developed ANN was trained on 4424 propeller designs. Similarly, Li et al. [23] developed data-driven surrogate model for the prediction of propeller open water characteristics. The authors identified eight input parameters that are relevant for the determination of propeller open water characteristics through correlation and importance analysis. The main finding of the study is that the support vector regression achieved the highest predictive accuracy on the validation dataset among the considered ML algorithms.

In the present study, a novel procedure for the preliminary design of marine propellers is proposed. An ANN, trained on experimentally obtained propeller open-water characteristics, is coupled with a GA to systematically determine the optimal propeller parameters that maximize  $\eta_o$  while simultaneously satisfying the prescribed design constraints. The proposed framework enables the direct identification of optimal propeller characteristics within the early design stage, thereby providing a structured and computationally efficient decision-support tool for designers. The developed procedure is demonstrated through selected case studies involving various hull forms of large commercial ships, confirming its robustness and broad applicability. The results further indicate that the ANN is capable of accurately reproducing propeller open water characteristics even when trained on a relatively limited set of experimental data, highlighting the practical feasibility of the proposed procedure as opposed to similar studies where a large database was used for the training of the ML models. To enable practical use of the proposed optimization procedure, a standalone application was developed in MATLAB that integrates the trained ANN with the GA optimization procedure within its graphical user interface. The installation files for the developed tool can be found at <https://github.com/carloggrlj/OptiProp>. The remainder of the paper is organized as follows: Section 2 describes in detail the procedure for developing the ANN and the optimization approach as well as the ships used as case studies. Section 3 presents the obtained results, and Section 4 summarizes the main findings of the study.

## 2. Methods

### 2.1 General overview

The aim of the present study is to obtain an optimal propeller for a ship with the known required thrust  $T$ , thrust deduction fraction  $t$ , wake fraction  $w$ , and propeller loading  $K_T / J^2$ . First an ANN is trained to develop a surrogate propeller model that takes the propeller main parameters, i.e.,  $P/D$ , hub ratio  $d/D$ ,  $A_E / A_0$ , and  $Z$  as inputs, and predicts  $K_T$  and  $K_Q$  over a range of advance coefficients  $J$ . Consequently, the  $\eta_o$  is calculated. The trained ANN is subsequently integrated into an optimization procedure based on GA. Within the optimization procedure, the propeller geometric characteristics are varied and  $\eta_o$  is obtained for

specific  $K_T / J^2$ . The objective is to obtain the propeller geometric characteristics that yield the maximum  $\eta_0$  while keeping the design variables within the bounds defined by the training dataset and enforcing cavitation and noise criteria through penalty terms. After the GA converges, the optimal propeller corresponding to the specified design speed is identified, its main geometric parameters are extracted, and the results are reported. Figure 1 illustrates schematically the proposed model.

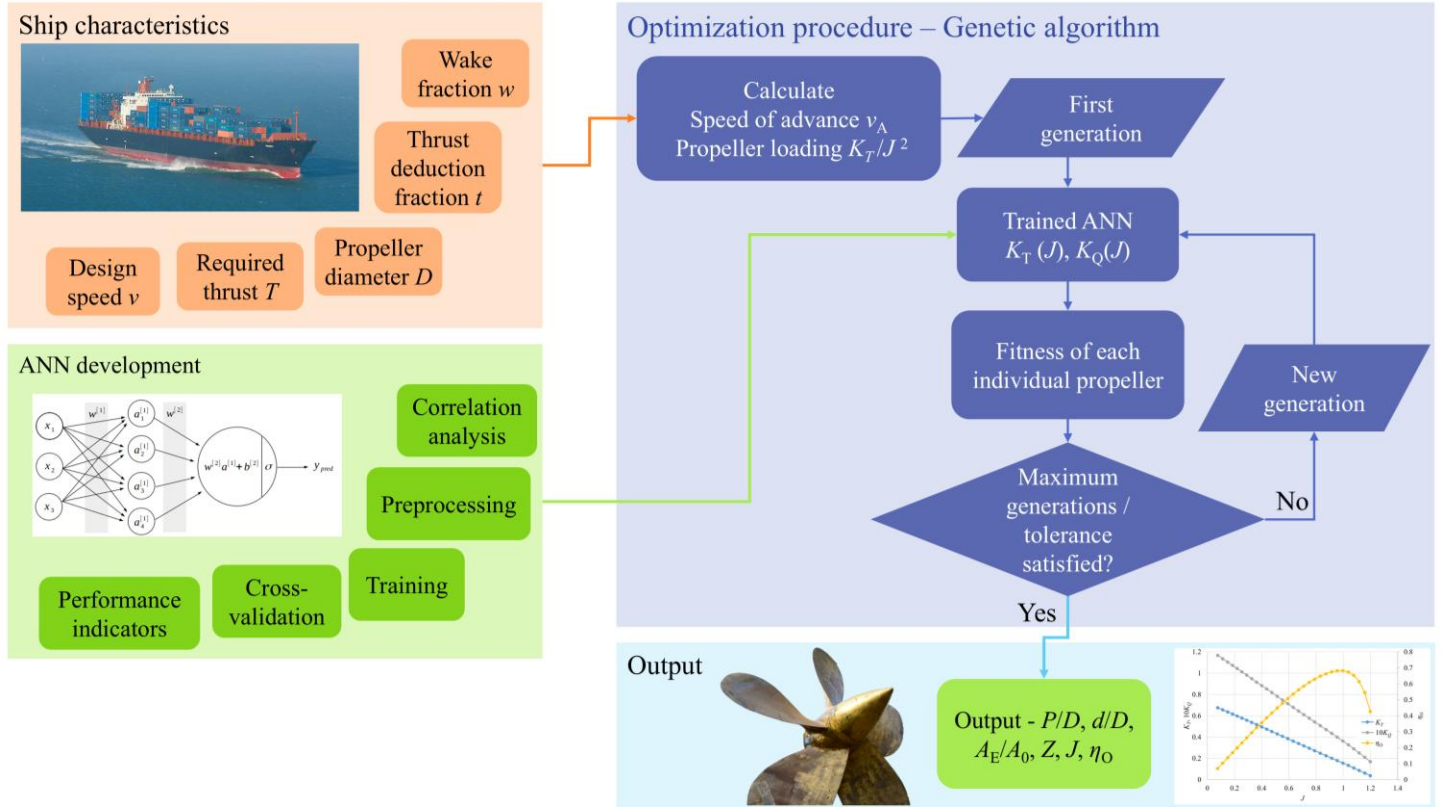


Fig. 1 A schematic illustration of the proposed numerical approach.

## 2.2 Database

The database used to develop the ANN is based on comprehensive open water tests conducted at the Brodarski Institute (Jadranbrod d.d.) in Zagreb. The open water test consists of the propeller model attached to a horizontal shaft, which is immersed at 1.5 times the propeller diameter  $D$  below the free surface. The test is conducted by maintaining the same rate of revolution  $n$  while varying the speed at which the propeller model is towed from 0 m/s until the thrust and torque become negative. During the experiment the following physical quantities were measured at each  $J$ : the towing speed, i.e. the speed of advance  $v_A$ , propeller thrust  $T$ , propeller torque  $Q$ , and  $n$  using the propeller dynamometer and a revolution counter. The  $K_T$  and  $K_Q$  are calculated for the entire range of  $J$  with the following expressions:

$$K_T = \frac{T}{\rho n^2 D^4} \tag{1}$$

$$K_Q = \frac{Q}{\rho n^2 D^5} \tag{2}$$

where  $\rho$  is the water density. Based on these physical parameters,  $J$  and  $\eta_0$  are calculated with the following expressions:

$$J = \frac{v_A}{nD} \tag{3}$$

$$\eta_o = \frac{K_T}{K_Q} \frac{J}{2\pi} \tag{4}$$

**Table 1** Descriptive statistics of propeller characteristics used as inputs

Value	Inputs			
	$P/D$	$d/D$	$A_E/A_0$	$Z$
Minimum	0.60	0.14	0.30	3.00
Mean	0.98	0.20	0.72	4.05
Median	0.89	0.19	0.65	4.00
Mode	1.00	0.19	1.05	4.00
Maximum	1.80	0.33	1.20	5.00
Standard deviation	0.29	0.05	0.23	0.67

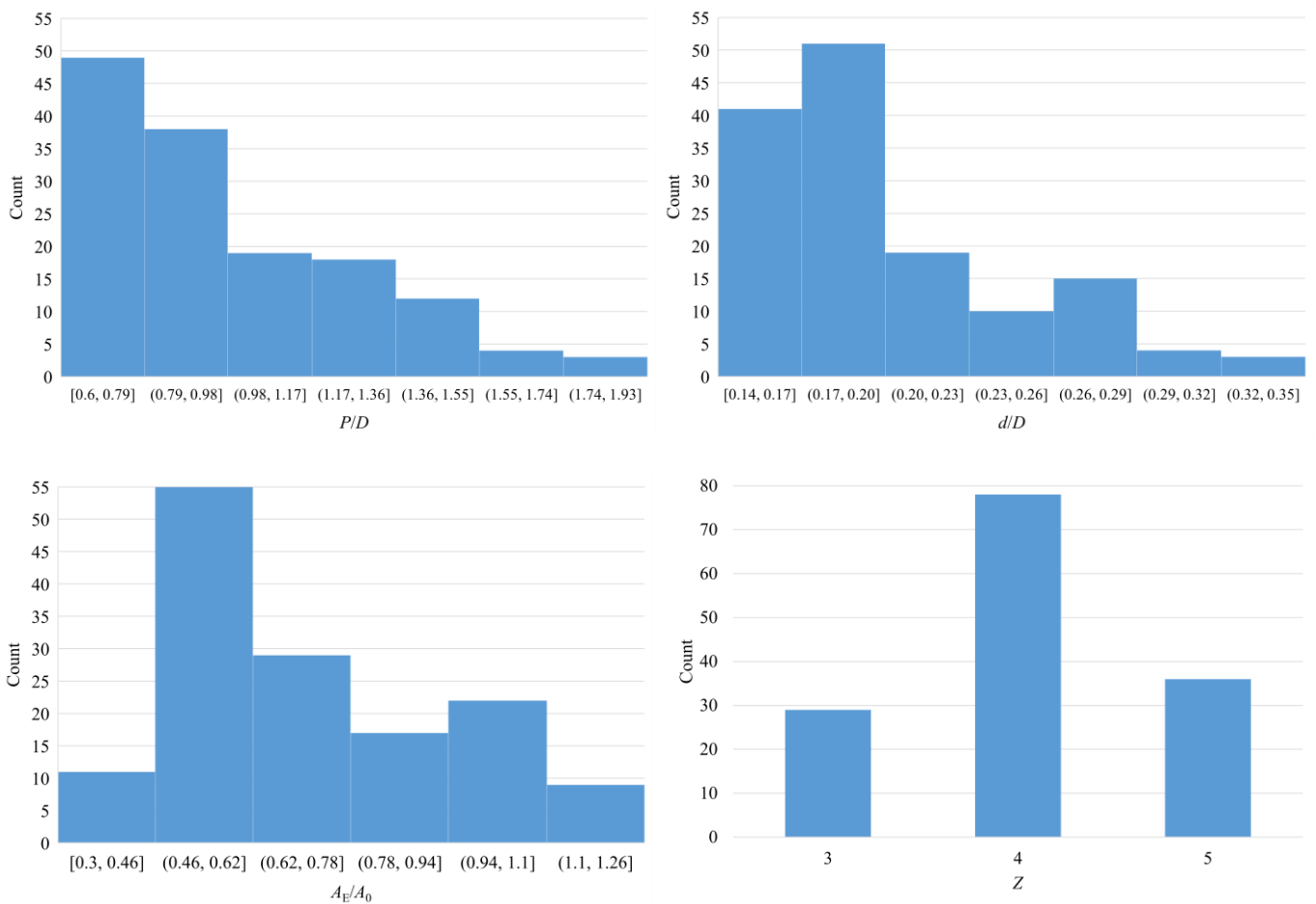


**Fig. 2** Histograms of the input variables

The descriptive statistics of propeller characteristics used as inputs can be seen in Table 1. A total of 143 propellers were used to establish the database, with each propeller providing  $K_T$  and  $K_Q$  values over a range of  $J$ . As shown in the histograms in Figure 2, most of the propellers have  $P/D$  between 0.6 and 0.98, and  $d/D$  between 0.14 and 0.2. As the values  $P/D$  and  $d/D$  increase, the number of propellers decrease. The number of propellers that have  $P/D > 1.55$  or  $d/D > 0.29$  is lower than 10. For most of the analysed propellers, the  $A_E/A_0$  ranges between 0.46 and 0.62, with only 10 propellers having  $A_E/A_0 < 0.46$ . At higher

$A_E / A_0$  the number of propellers also decreases. Among the 143 propellers, 78 have four blades, 36 have five blades, and 29 have three blades.

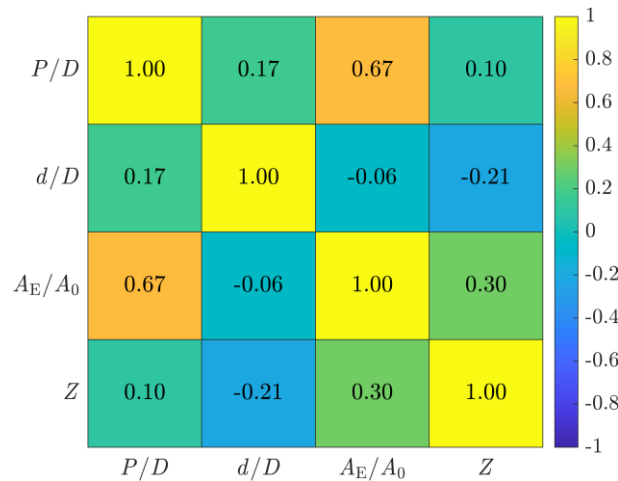


**Fig. 3** The correlation matrix of input variables

The results of the correlation analysis presented in Figure 3 shows that most input variables are largely independent, which is beneficial for ANN modelling and reduces the risk of multicollinearity. The strongest correlation observed is between  $P/D$  and  $A_E / A_0$ , indicating a moderate-to-strong positive relationship where higher pitch ratios tend to coincide with larger expanded area ratios.  $P/D$  also has very weak positive correlations with  $d/D$  and  $Z$ , suggesting minimal association with hub-to-diameter ratio and number of blades.  $A_E / A_0$  and  $d/D$  are essentially uncorrelated, while  $Z$  shows a weak negative correlation with  $d/D$  and a weak positive correlation with  $A_E / A_0$ , indicating that the number of blades varies slightly with these geometric parameters but remains largely independent. Overall, the results suggest that the input variables are mostly uncorrelated, which supports robust ANN training and implies that the network can learn the influence of each parameter on the outputs without strong redundancy among inputs.

The scatter diagrams presented in Figure 4 indicate that  $P/D$  spans a relatively wide range, however, most propellers are concentrated within the lower-to-moderate interval, with comparatively fewer high pitch designs. As previously noted,  $d/D$  is largely confined between 0.14 and 0.20. The distribution of  $A_E / A_0$  shows that medium-area designs predominate within the dataset.

Prior to the training process, the dataset was carefully examined to identify potential outliers, and inconsistencies. Particular attention was given to  $K_T$  and  $K_Q$  across the range of  $J$ . Data points exhibiting non-physical behaviour or clear deviation from expected propeller performance characteristics were excluded from the database. This preprocessing step ensured a consistent, physically meaningful, and reliable dataset, thereby improving the robustness, stability, and predictive capability of the ANN. From the initial 147 propellers, a total of 143 propellers were considered in the study.

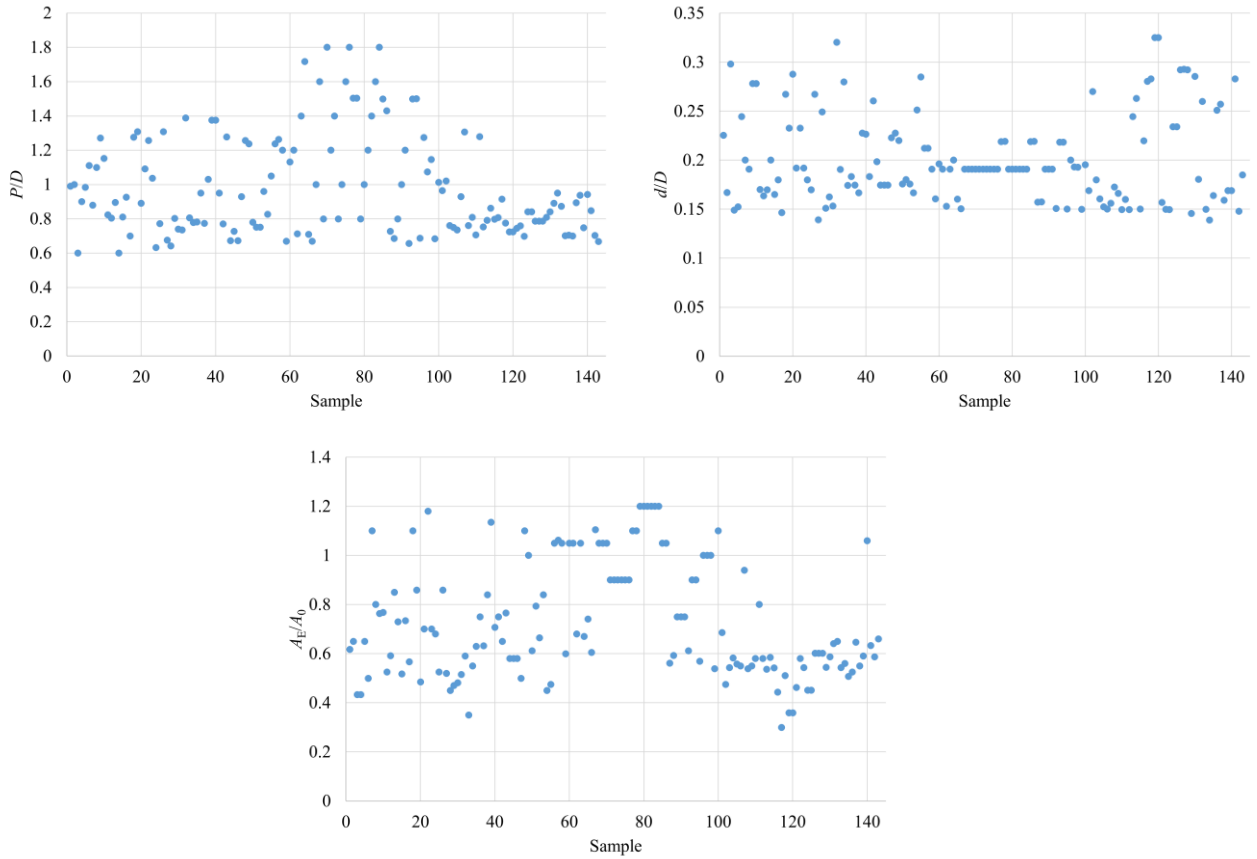


**Fig. 4** Scatter diagrams of the input variables

### 2.3 Artificial neural network

The ANN was developed to predict  $K_T$  and  $K_Q$  as functions of  $J$  based on the four previously defined geometric input parameters. Since the propellers were not experimentally tested at an identical number of  $J$  values during the open water tests, the output data were resampled prior to training to ensure that each propeller was represented by an output matrix of uniform dimensions. Resampling was performed using linear interpolation at 30 points for each propeller. The output matrix consists of  $K_T$  and  $K_Q$  values and the respective  $J$  values. Both input and output variables were standardized before the training process to eliminate differences in numerical scale and to ensure that the ANN learned the underlying physical relationships rather than being influenced by magnitude disparities among variables. Initially, four training algorithms were evaluated: Levenberg-Marquardt, scaled conjugate gradient, resilient backpropagation, and Levenberg-Marquardt with Bayesian regularization. The investigated ANN architectures consisted of a single hidden layer with 5, 10, 15, or 20 neurons. Additionally, three activation functions within the neurons in hidden layer were examined:

- Rectified Linear Unit (ReLU):

$$y = \text{ReLU}(x) = \begin{cases} x, & x > 0 \\ 0, & x \leq 0 \end{cases} \quad (5)$$

- Hyperbolic tangent:

$$y = \frac{e^x - e^{-x}}{e^x + e^{-x}} \quad (6)$$

- Sigmoid:

$$y = \frac{1}{1 + e^{-x}} \quad (7)$$

In supervised learning, the neural network receives input data along with the corresponding target outputs. The predicted outputs are compared to the target values, and a learning algorithm iteratively adjusts the network weights and biases to reduce the discrepancy between them. This process aims to minimize the defined error function by progressively refining the network parameters. A 5-fold cross-validation procedure was applied to assess model performance more reliably. The complete dataset was partitioned into five equally sized subsets. The training and validation process was repeated five times, each time using one subset as the validation set and the remaining four subsets for training. The final performance indicators were obtained by averaging the results over all five folds. The following metrics have been computed:

- Coefficient of determination:

$$R^2 = 1 - \frac{\sum_{i=1}^n (y_i - y'_i)^2}{\sum_{i=1}^n (y_i - \bar{y}_i)^2} \quad (8)$$

- Root Mean Squared Error:

$$RMSE = \sqrt{\frac{\sum_{i=1}^n (y_i - y'_i)^2}{n}} \quad (9)$$

where  $y_i$  is the actual value,  $y'_i$  is the predicted value,  $\bar{y}_i$  is the mean of the actual values, and  $n$  is the total number of samples.

#### 2.4 Optimization study

The optimization procedure is implemented by employing the GA within the software package MATLAB 2025b [24]. The GA is a population-based evolutionary optimization method inspired by natural selection mechanisms. It consists of a population of candidate solutions, also called individuals, each representing a feasible combination of propeller design variables. For each generation, the fitness of all individuals is evaluated using the trained ANN, which predicts the corresponding open water characteristics. Based on the assigned fitness values, individuals with superior performance are selected to form the next generation. Genetic operators, including crossover and mutation are applied to the selected parent individuals to generate offspring. In this study, the GA is used to identify a surrogate propeller with the maximum  $\eta_o$ . The optimization procedure is conducted subject to the cavitation constraint imposed by Keller's criterion [1], which prescribes a minimum allowable  $A_E / A_0$  to ensure adequate cavitation performance as well as the noise criterion, which prescribes a maximal propeller tip speed  $v_{tip}$ .

The optimization process is defined by minimising an objective function as follows:

$$\min_x f(x) \text{ such that } \begin{cases} c(x) \leq 0 \\ c_{eq}(x) = 0 \\ A \cdot x \leq b \\ A_{eq} \cdot x = b_{eq} \\ lb \leq x \leq ub \end{cases} \quad (10)$$

where  $x$  is the input vector,  $f(x)$  is the objective function,  $c$  and  $c_{eq}$  are the inequality and equality constraints, respectively,  $A$  and  $b$  form the linear inequality constraints, while  $A_{eq}$  and  $b_{eq}$  form the linear

equality constraints, lb and ub are the lower and upper bounds, respectively. In this study, the equality and inequality constraints are not used, only the lower and upper bounds are defined for each design variable.

The fitness function is defined by combining the objective, the Keller's cavitation [25], and noise constraints as penalties. This way, both the objective and constraints are evaluated in a single equation [26]. Consequently, the problem can be interpreted as an unconstrained optimization with bound constraints, where infeasible solutions are discouraged via penalization rather than strict constraint handling. The fitness function reads as follows:

$$\begin{aligned} \text{fitness function} = \eta_O + w_{\text{Keller}} \cdot \max[0, (A_E / A_0)_{\min} - (A_E / A_0)] + \\ + w_{\text{tip, speed}} \cdot \max(0, v_{\text{tip}} - v_{\text{tip, max}}) \end{aligned} \quad (11)$$

where  $w_{\text{Keller}}$  and  $w_{\text{tip, speed}}$  are the cavitation and noise constraint penalty weights, respectively, while the minimum expanded area ratio  $(A_E / A_0)_{\min}$  and  $v_{\text{tip}}$  are defined as:

$$(A_E / A_0)_{\min} = \frac{(1.3 + 0.3Z)T}{(p_{\text{atm}} + \rho g h_0 - p_v)D^2} + K \quad (12)$$

$$v_{\text{tip}} = Dn\pi \quad (13)$$

where  $n$  is the calculated rate of revolution of the considered propeller using  $v_A$  for the specific ship,  $p_{\text{atm}}$  is the atmospheric pressure,  $h_0$  is the immersion depth of the propeller shaft and  $K$  is the constant equal to 0.2 for the single-screw ships. The Keller's cavitation constraint simply states that the  $A_E / A_0$  must be higher than the  $(A_E / A_0)_{\min}$  as calculated with Equation (12). To satisfy the noise constraint, the  $v_{\text{tip}}$  must be below the maximum value as defined by Tadros et al. [3]: maximum tip speed for three- and four-bladed propellers is equal to 53 m/s while for five-bladed propellers is equal to 46 m/s.

Based on a preliminary sensitivity analysis, the population size was set to 100 and the function tolerance equal to  $10^{-4}$ . The maximum number of generations was set as 500, although the simulation stopped much earlier due to the satisfaction of the function tolerance. To avoid the local optima, the GA was performed 10 times in a row. The number of iterations was set to 10, as further repetitions did not yield any significant improvement in the results, indicating convergence. Other GA parameters were set to MATLAB default values: a crossover fraction of 0.8, an elite count of 5 (the number of individuals guaranteed to survive to the next generation), a Gaussian mutation function, and the *selectiontournament* selection method.

## 2.5 Case studies

The hull forms used in the optimization study are presented in Figures 5 and 6, while the respective main particulars are listed in Table 2. Ships considered in this study are as follows: KCS, Japan Bulk Carrier (JBC), post-Panamax 6750 TEU containership, and Duisburg Test Case (DTC). In the following subsections, each ship is briefly described and the source of input parameters for the present study are given.

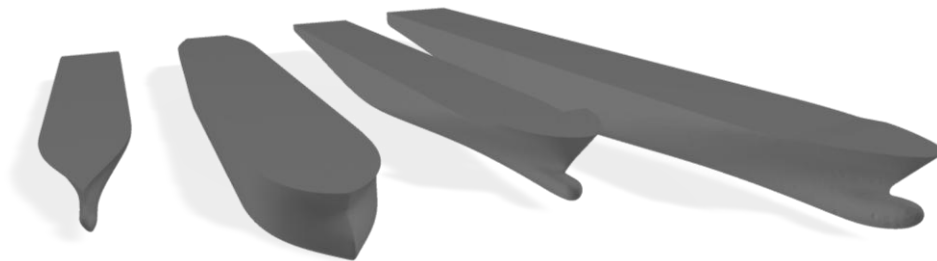


**Fig. 5** Ships considered in the optimization study, left to right – KCS, JBC, 6750 TEU containership, DTC



**Fig. 6** Side view of the ships considered in the optimization study

**Table 2** Main particulars of the ships

Main particular	KCS	JBC	6750 TEU containership	DTC
Length between perpendiculars $L_{pp}$ , m	230	280	286.6	355
Length of waterline $L_{WL}$ , m	233.54	285	292.5	356.1
Length overall $L_{OA}$ , m	243	291	304	372.8
Breadth $B$ , m	32.2	45	40	51
Draught $T$ , m	10.8	16.5	11.98	14.5
Displacement $\nabla$ , m <sup>3</sup>	52,030	178,420.1	85,562.7	173,467
Propeller shaft immersion $h_0$ , m	6.7	11.32	8.06	9.5
Propeller diameter $D$ , m	7.9	8.12	7.3	8.91
Design speed $V$ , kn	24	14.5	23	25

### 2.5.1 KRISO containership

The KCS is a 3600 TEU containership developed by KRISO for the International Workshop on CFD in Ship Hydrodynamics in Gothenburg 2000 [27]. Since then, it was used in various experimental and numerical studies. One such study was conducted by Farkas et al. [28], in which the authors performed full-scale numerical simulations of the resistance, open water, and self-propulsion tests for the KCS equipped with the KP505 propeller. The numerical results obtained for the smooth surfaces were used in this study as an input for the optimization study. Also, the required propulsion characteristics were calculated using the Holtrop-Mennen method [29].

### 2.5.2 Japan Bulk Carrier

The second case study is the JBC which is a benchmark ship developed by the National Maritime Research Institute at the Yokohama National University, and the Ship Building Research Centre of Japan for the CFD workshop in 2015 [30]. It is a bulk carrier with a high block coefficient that consists of a bulbous bow and a transom stern. The JBC was a part of the experimental campaign lead at the Brodarski Institute (Jadranbrod d.d.) in Zagreb [31], and the experimental results were published by Degiuli et al. [32]. The experimental campaign was conducted as a part of the Croatian Science Foundation research project “Sustainable slow steaming for low carbon shipping, IP-2020-02-8568 (STARSHIP)” and consisted of resistance, self-propulsion, open water tests as well as the measurements of the nominal wake. For this study, the required input data for the optimization procedure were obtained from the full-scale numerical results

provided by Grlj et al. [33, 34], the extrapolated towing tank measurements published by Degiuli et al. [27], as well as from calculations performed using the method proposed by Holtrop and Mennen [29].

### 2.5.3 Post-Panamax 6750 TEU containership

The third case study is the post-Panamax 6750 TEU containership which is a benchmark containership developed for the assessment of the performance of the seakeeping analysis codes as a part of the ITTC-ISSC joint workshop in 2014 [35]. This containership was also investigated in an experimental campaign performed at the Brodarski Institute (Jadranbrod d.d.) [36] by Degiuli et al. [37], where its hydrodynamic characteristics were assessed through resistance, open water, and self-propulsion tests. The experimental campaign was conducted as a part of the Croatian Science Foundation research project “Sustainable slow steaming for low carbon shipping, IP-2020-02-8568 (STARSHIP)”. For this study, the required input data for the optimization procedure were obtained from the full-scale numerical results provided by Grlj et al. [38], the extrapolated towing tank measurements published by Degiuli et al. [37], as well as from calculations performed using the method proposed by Holtrop and Mennen [29].

### 2.5.4 Duisburg Test Case

Finally, the DTC is a 14000 TEU post-Panamax containership developed at the Institute of Ship Technology, Ocean Engineering and Transport Systems [39]. It represents a benchmark case that has been widely used in previous experimental investigations and for the validation of numerical results. It is a single-screw ship with a bulbous bow, large stern overhang and a transom. To assess the hydrodynamic performance of DTC, Farkas et al. [40] conducted numerical simulations of the resistance, open water, and self-propulsion tests. The published numerical results were used in this study, alongside the calculated results with the Holtrop-Mennen method [29] and experimental data provided by Moctar et al. [39].

## 3. Results and discussion

### 3.1 Artificial neural network

The ANN trained with Levenberg-Marquardt algorithm using Bayesian regularization demonstrated superior performance compared to the other evaluated learning algorithms, consistent with findings from similar studies [3, 41]. It incorporates a penalty on large network weights directly into the training objective, serving as a built-in regularization mechanism that helps prevent overfitting, which is a common issue with small datasets such as the one used within this study. By balancing network complexity against the training error, it produces models that generalize more effectively to unseen data. Another advantage is that all available data can be used for training without requiring a separate test set, maximizing the information available to the network, an especially valuable feature when working with small datasets. The issue of overfitting with the other learning algorithms was apparent, as the predicted  $K_T$  and  $K_O$  curves lacked smoothness. The best-performing topology was found to have 10 neurons in the hidden layer, using the ReLU activation function. The optimal ANN achieved an  $R^2$  of 0.961 on the training set and 0.951 on the validation set. The  $RMSE$  values for the training and validation datasets are 0.197 and 0.2029, respectively. Although networks with a larger number of neurons in the hidden layer produced a training  $R^2$  exceeding 0.99, their validation set  $R^2$  was substantially lower than that of the optimal model, indicating overfitting.

Figures 7 and 8 present the comparison between predicted and experimentally measured values  $K_T$  and  $K_O$ , respectively, for two representative advance ratios,  $J = 0.3$  and  $J = 0.6$ . Overall, the predicted results show strong agreement with the corresponding experimental data. With the exception of a small number of outliers, the majority of data points are closely clustered around the line of perfect agreement, indicating that the model captures the underlying trends with a high degree of accuracy. The dispersion remains limited across both advance ratios, demonstrating consistent predictive capability over different operating regimes.

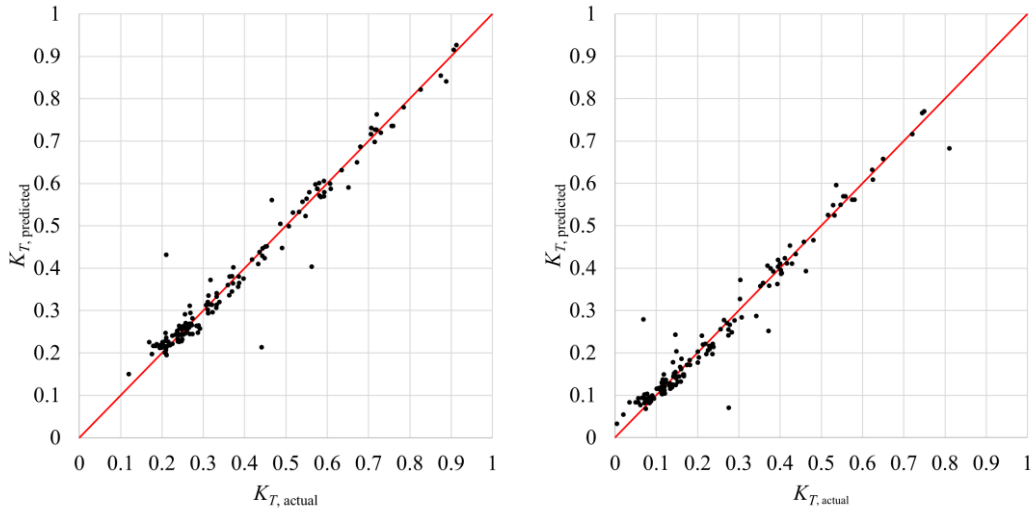


**Fig. 7** Predicted vs. actual values for  $K_T$  for  $J = 0.3$  (left) and  $J = 0.6$  (right)

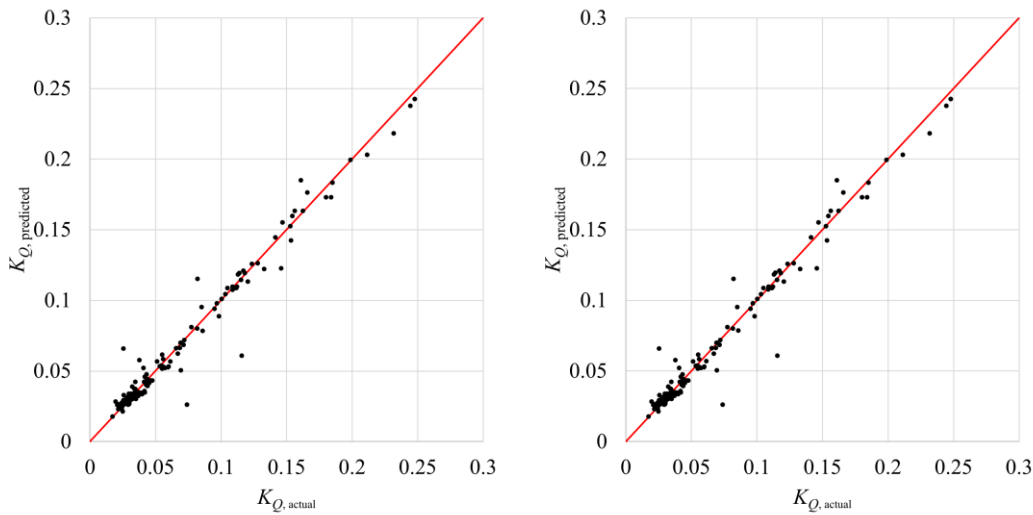


**Fig. 8** Predicted vs. actual values for  $K_Q$  for  $J = 0.3$  (left) and  $J = 0.6$  (right)

The open water curves of the original DTC propeller were predicted using the developed ANN. A comparison between the experimentally obtained open water curves and those predicted by the trained ANN is presented in Figure 9. The ANN predicts slightly higher  $K_Q$  values compared to the experimental data, while the discrepancies in the  $K_T$  curves are negligible, with only minor differences observed at lower  $J$  values. As a result, the predicted  $\eta_o$  is slightly lower than the experimental value. This analysis demonstrates that the developed ANN is capable of predicting open water curves with satisfactory accuracy, even for a propeller that was not included in the training or validation sets.

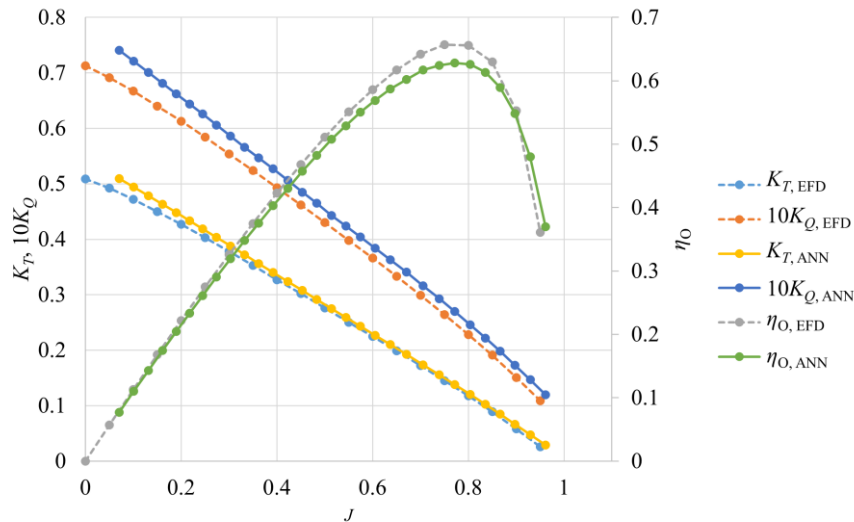


**Fig. 9** Comparison between the experimentally obtained open water curves and those predicted by the developed ANN for the DTC

**Table 3** Input parameters for the different ships

	KCS			JBC			6570 TEU containership			DTC		
	EFD	CFD	Holtrop	EFD	CFD	Holtrop	EFD	CFD	Holtrop	EFD	CFD	Holtrop
$T$ , kN	1757	1570	1879	1583	1383	1309	1959	1783	2005	3659	3705	4178
$t$	0.147	0.133	0.165	0.124	0.270	0.208	0.160	0.158	0.176	0.090	0.110	0.195
$w$	0.197	0.227	0.218	0.490	0.360	0.583	0.271	0.275	0.222	0.187	0.195	0.294
$K_T / J^2$	0.327	0.310	0.377	1.847	1.229	2.519	0.482	0.527	0.525	0.451	0.476	0.772

### 3.2 Optimization study

The input data for the optimization study are  $T$ ,  $t$ ,  $w$ , and  $K_T / J^2$  (Table 3) along with the seawater density  $\rho = 1026 \text{ kg/m}^3$ ,  $V$ ,  $D$ , and  $h$ , Table 2. It can be noticed that the different methods yield different results as expected. The biggest differences are obtained for DTC, where Holtrop-Mennen method predicts the highest  $T$ . The input data obtained for KCS and the post-Panamax 6750 TEU containership are the most consistent across different methods.

After completing the optimization procedure, the optimal propellers are identified and their corresponding geometric and open water characteristics are summarized in Tables 4-7, together with comparisons against the original propellers for each ship. For most ships, the highest  $\eta_0$  is obtained when CFD-derived input data are used, whereas for the DTC the maximum  $\eta_0$  is achieved using EFD data. When Holtrop-Mennen method is used for the input data, the optimal  $\eta_0$  are lower than those of the original propellers except for the post-Panamax 6750 TEU containership where a slightly higher  $\eta_0$  is obtained. Similar results are obtained when EFD-derived input data is used. The optimal  $d / D$  remain close to those of the original propellers, while  $P / D$  are generally larger than those of the original propellers, with some deviations observed for the JBC. When the input parameters are determined using the Holtrop-Mennen method, both the achieved  $\eta_0$  and the corresponding geometric characteristics are lower than those obtained using CFD or EFD data, as well as lower than those of the original propellers. The optimal  $Z$  is consistently equal to five for all the considered ships, except for the JBC with the Holtrop-Mennen method where the optimization procedure yields a four-bladed propeller. For the post-Panamax 6750 TEU containership, the optimization procedure yields a five-bladed propeller with all the methods applied for obtaining the input data, whereas the original design features four blades. Since propeller performance is strongly influenced by the

wake fraction, the significant differences in the obtained geometric parameters can be attributed to variations in the wake fraction predicted by different methods. The smallest differences in wake fraction are observed for the KCS and the post-Panamax 6750 TEU containership. Consequently, the optimized geometric parameters are consistent for these cases. In contrast, the JBC and DTC results exhibit significant differences in wake fraction, which leads to corresponding variations in the optimal propeller.

**Table 4** Original and optimal propeller obtained for KCS with different input data

	Original	EFD	CFD	Holtrop
$P/D$	0.997	1.1855	1.1855	1.1855
$d/D$	0.180	0.1932	0.1932	0.1932
$A_E/A_0$	0.800	0.7552	0.7384	0.8884
$Z$	5	5	5	5
$J$	0.679	0.8344	0.8432	0.8217
$K_T$	0.195	0.2278	0.2209	0.2544
$K_Q$	0.032	0.0458	0.0446	0.0516
$\eta_o$	0.650	0.6599	0.664	0.6452

**Table 5** Original and optimal propeller obtained for JBC with different input data

	Original	EFD	CFD	Holtrop
$P/D$	0.736	1.1057	1.1855	0.6904
$d/D$	0.190	0.1936	0.1930	0.1618
$A_E/A_0$	0.640	0.6884	0.7384	0.4954
$Z$	5	5	5	4
$J$	0.351	0.4510	0.5539	0.2921
$K_T$	0.199	0.3756	0.3769	0.2149
$K_Q$	0.026	0.0599	0.0665	0.0244
$\eta_o$	0.452	0.4502	0.4998	0.4101

**Table 6** Original and optimal propeller obtained for post-Panamax 6750 TEU containership with different input data

	Original	EFD	CFD	Holtrop
$P/D$	0.890	1.1855	1.1855	1.1602
$d/D$	0.169	0.1932	0.1932	0.1905
$A_E/A_0$	0.750	0.8884	0.8884	0.9884
$Z$	4	5	5	5
$J$	0.622	0.7307	0.7495	0.7488
$K_T$	0.186	0.3065	0.2957	0.2944
$K_Q$	0.029	0.0595	0.0579	0.0581
$\eta_o$	0.603	0.5986	0.6093	0.6035

**Table 7** Original and optimal propeller obtained for DTC with different input data

	Original	EFD	CFD	Holtrop
$P/D$	0.959	1.1602	1.1602	1.2145
$d/D$	0.176	0.1905	0.1905	0.1886
$A_E/A_0$	0.800	0.9884	0.9884	1.1884
$Z$	5	5	5	5
$J$	0.615	0.7814	0.77	0.6782
$K_T$	0.316	0.2756	0.2822	0.3548
$K_Q$	0.054	0.0552	0.0562	0.0724
$\eta_o$	0.592	0.6207	0.6148	0.5291

Overall, the optimized propellers demonstrate higher  $A_E/A_0$  compared to the original ones, which is in agreement with the findings from Tadros et al. [3]. In particular, the results obtained for the KCS show close agreement with those reported by Tadros et al. [3]. The optimized KCS propeller exhibits higher  $\eta_o$ ,  $P/D$ , and  $A_E/A_0$  compared to the original propeller. These results indicate that an optimal propeller design can be successfully obtained using an ANN trained on a relatively small dataset.

Finally, the obtained open water curves for each ship using the input data from CFD are presented in Figure 9. It can be observed that the obtained values of  $K_T$ ,  $K_Q$ , and  $\eta_o$  for each ship are smooth and free of outliers, indicating that the ANN does not exhibit overfitting and demonstrates strong generalization capability. The open water curves for KCS and JBC are similar since the obtained optimal propellers have similar geometric parameters. A similar trend is observed for the post-Panamax 6750 TEU containership and the DTC, whose optimized propellers also yield closely matching open water curves.

To facilitate the practical implementation of the proposed optimization procedure, a standalone application called OptiProp was developed using MATLAB App Designer within the software package MATLAB. The application integrates the trained ANN with the optimization procedure based on GA into a user-friendly graphical interface. It enables the user to define the ship propulsion characteristics and its operating conditions. After the calculations are performed, the results are shown within the same graphical interface. The tool provides the propeller geometric parameters, open water characteristics, including  $K_T$ ,  $K_Q$ , and  $\eta_o$  in a table and plots the curves in a diagram. Figure 10 shows the graphical interface of the developed application, where the input and output can be seen.

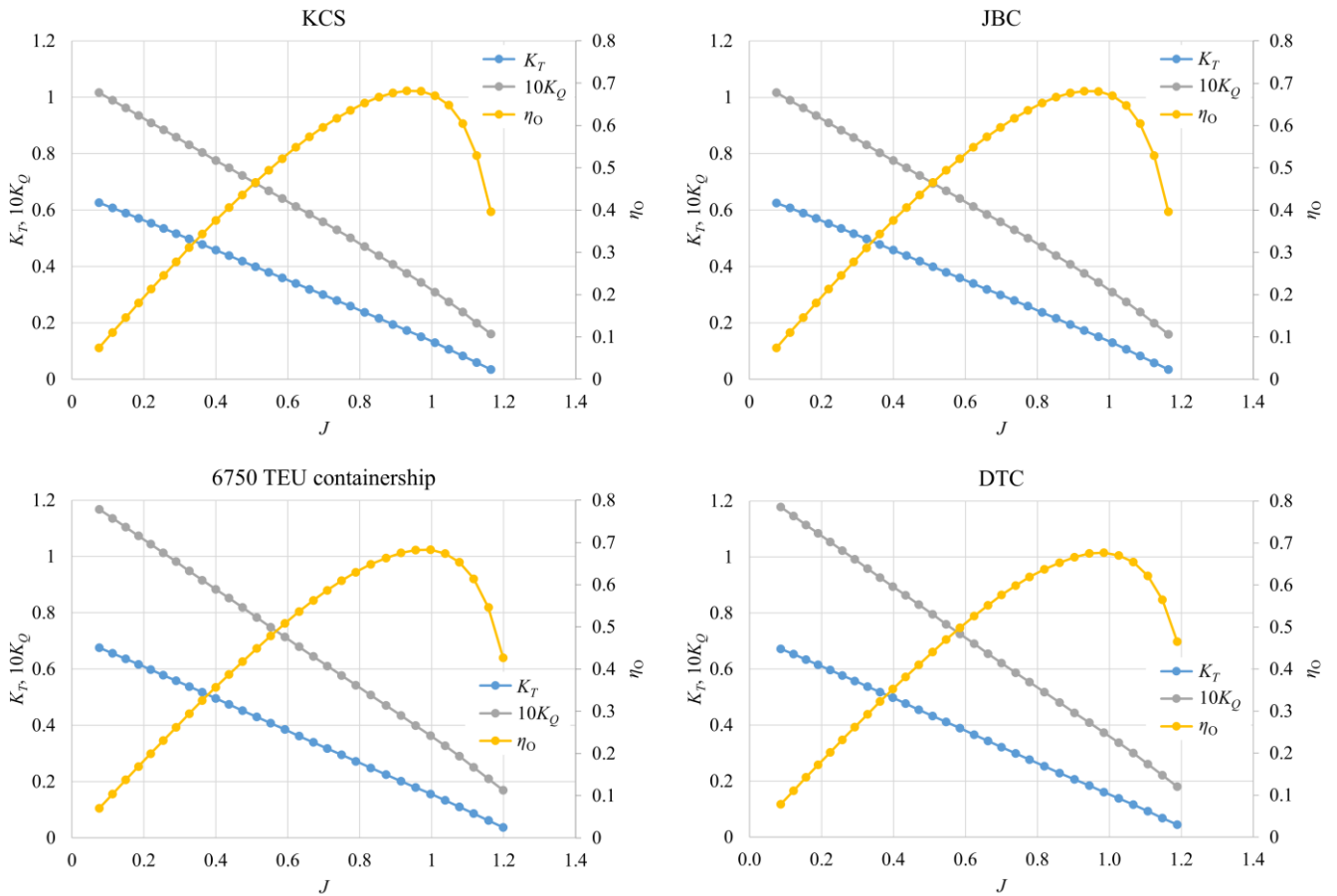


Fig. 9 Open water curves obtained for each case study using the input data from CFD

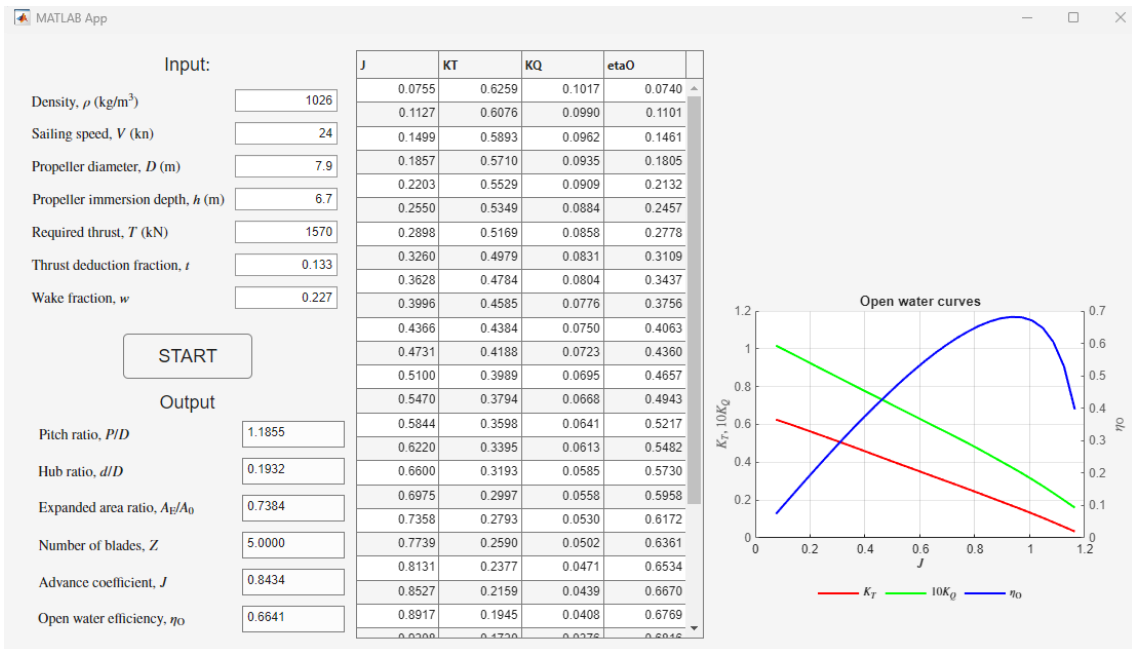


Fig. 10 The OptiProp graphical interface

### 4. Conclusions

In this study, a numerical approach is proposed for the determination of a propeller characteristics with maximum open water efficiency for a given ship, taking into account its propulsion characteristics and

prescribed operating conditions. The methodology combines a data-driven surrogate model based on an artificial neural network with an optimization procedure employing the genetic algorithm. The artificial neural network is trained on experimentally obtained open water characteristics of 143 various propeller designs, with the dataset provided by the Brodarski Institute (Jadranbrod d.d.). By learning the relationship between key geometric parameters and the resulting thrust and torque coefficients, the artificial neural network serves as a fast and reliable surrogate model suitable for optimization procedure.

The trained artificial neural network is subsequently integrated into an optimization procedure based on genetic algorithm, enabling efficient exploration of the design space while satisfying the imposed design and operational constraints. The results demonstrate that the proposed approach can successfully identify propellers with higher open water efficiency compared to the original ones. In particular, the results obtained for the KRISO containership show close agreement with those reported by Tadros et al. [3], despite the significantly smaller training dataset used in the present study. This confirms that satisfactory and practically relevant results can be achieved even when the artificial neural network is trained on a relatively limited number of experimental data.

An additional advantage of the proposed approach lies in its flexibility with respect to input data source. The propulsion characteristics required for the optimization procedure can be obtained from various sources, including high-fidelity numerical simulations and towing tank tests, or low-fidelity empirical prediction methods. In this study, input data were derived from both numerical and experimental investigations, as well as from calculations based on the empirical method proposed by Holtrop and Mennen. The results indicate that the optimization framework remains applicable and robust across different levels of input-data fidelity, highlighting its potential as a practical tool for preliminary propeller design.

Finally, a standalone application named *OptiProp*, was developed in MATLAB to integrate the trained artificial neural network and optimization procedure based on the genetic algorithm into a graphical interface. The installation files for the developed tool can be found at <https://github.com/carloggrlj/OptiProp>. The tool allows the user to define the ship propulsion characteristics and operating conditions, executes the optimization process, and presents the optimized propeller geometric parameters together with the predicted open water characteristics in both tabular and graphical form, thereby facilitating the practical implementation of the proposed method.

The scientific contributions of this study can be summarized as follows:

- An artificial neural network is developed as a surrogate model based on experimental data, rather than on systematic series data.
- A comparative analysis of optimal propellers obtained with different input data is presented.
- A standalone optimization tool, *OptiProp*, is developed based on the proposed methodology.

This study demonstrates that optimal propeller designs can be obtained for the design operating condition using the proposed method. The same approach can be extended to other loading conditions or operating speeds, provided that appropriate input data are available. Additionally, the training database for the artificial neural network can be expanded to include a wider range of propellers. Finally, the performance of the optimized propellers should be validated through detailed numerical simulations or experimental investigations, such as self-propulsion tests.

## ACKNOWLEDGEMENTS

This work was supported by the Croatian Science Foundation under the project number IP-2025-02-4779.

## FUNDING

This work was funded by the Croatian Science Foundation under the project number IP-2025-02-4779.

## REFERENCES

- [1] Carlton, J., 2018. Marine Propellers and Propulsion. *Butterworth-Heinemann*.

- [2] Oosterveld, M.W.C., van Oossanen, P., 1975. Further computer-analyzed data of the Wageningen B-screw series. *International Shipbuilding Progress*, 22, 251-262. <https://doi.org/10.3233/ISP-1975-2225102>
- [3] Tadros, M., Shi, W., Xu, Y., Song, Y., 2024. A unified cross-series marine propeller design method based on machine learning. *Ocean Engineering*, 314, 119691. <https://doi.org/10.1016/j.oceaneng.2024.119691>
- [4] Martić, I., Degiuli, N., Grlj, C.G., 2023. Prediction of Added Resistance of Container Ships in Regular Head Waves Using an Artificial Neural Network. *Journal of Marine Science and Engineering*, 11(7), 1293. <https://doi.org/10.3390/jmse11071293>
- [5] Ao, Y., Li, S., Li, Y., Gong, J., 2024. The construction of a neural network proxy model for ship hull design based on multi-fidelity datasets and the parameter freezing strategy. *Journal of Marine Engineering & Technology*, 23, 270-280. <https://doi.org/10.1080/20464177.2024.2330174>
- [6] Lee, M.-K., Lee, I., 2023. Optimal Design of Flow Control Fins for a Small Container Ship Based on Machine Learning. *Journal of Marine Science and Engineering*, 11(6), 1149. <https://doi.org/10.3390/jmse11061149>
- [7] Degiuli, N., Grlj, C.G., Martić, I., Baressi Šegota, S., Anđelić, N., Majnarić, D., 2025a. Machine Learning Models for the Prediction of Wind Loads on Containerships. *Journal of Marine Science and Engineering*, 13(3), 417. <https://doi.org/10.3390/jmse13030417>
- [8] Grlj, C.G., Degiuli, N., Tuković, Ž., Farkas, A., Martić, I., 2023b. The effect of loading conditions and ship speed on the wind and air resistance of a containership. *Ocean Engineering*, 273, 113991. <https://doi.org/10.1016/j.oceaneng.2023.113991>
- [9] Yang, Z., Xu, Y., Jing, J., Fu, X., Wang, B., Ren, H., Zhang, M., Sun, T., 2023. Investigation of physics-informed neural networks to reconstruct a flow field with high resolution. *Journal of Marine Science and Engineering*, 11(11), 2045. <https://doi.org/10.3390/jmse11112045>
- [10] Tong, Z., Chen, R., 2026. Physics-informed spatiotemporal neural network for unsteady propeller wake prediction via least squares finite-difference framework. *Physics of Fluids*, 38(2), 025132. <https://doi.org/10.1063/5.0311065>
- [11] Bourchas, O., Papalambrou, G., 2025. Physics informed neural networks for vessel main engine power prediction. *Ocean Engineering*, 332, 121344. <https://doi.org/10.1016/j.oceaneng.2025.121344>
- [12] Hadavi, M., Akbarivakilabadi, K., Nikabadi, S., Ghasri, M., 2025. Data-Driven Structural and Aerodynamic Optimization of Ship Masts Using ANN-GA Framework Integrated with FEA and CFD Analysis. *Engineering Reports*, 7, e70362. <https://doi.org/10.1002/eng2.70362>
- [13] Lefkiou, C., Koukouvinis, P., Chatzis, S., Xyfolis, S., 2026. Predicting ship hull flow-field distributions using a soft-constrained ANN model. *International Journal of Naval Architecture and Ocean Engineering*, 18, 100712. <https://doi.org/10.1016/j.ijnaoe.2025.100712>
- [14] Cheng, X., Huang, X., Xu, D., Zhao, Z., Liu, H., Kong, M., Ji, R., 2024. Ship Optimization Based on Fully-Parametric Models for Hull, Propeller and Rudder. *Journal of Marine Science and Engineering*, 12(9), 1635. <https://doi.org/10.3390/jmse12091635>
- [15] Liu, J., Yue, Q., Wu, S., Yue, X., 2024. Hydrodynamic shape optimization of an autonomous and remotely-operated vehicle via a multi-surrogate model. *Brodogradnja*, 75(3), 75301. <https://doi.org/10.21278/brod75301>
- [16] Guo, S., Zhang, B., Tian, Z., Liu, J., Tang, H., 2024. Automatic Optimal Design Method for Minimum Total Resistance Hull Based on Enhanced FFD Method. *Brodogradnja*, 75(4), 75407. <https://doi.org/10.21278/brod75407>
- [17] Zhao, Y., Yu, M.H., Yuan, W., Su, Z., Shen, C.W., 2026. Research on a novel hull, main engine and propeller matching design framework. *Results in Engineering*, 29, 109296. <https://doi.org/10.1016/j.rineng.2026.109296>
- [18] Vázquez-Santos, A., Camacho-Zamora, N., Hernández-Hernández, J., Herrera-May, A.L., Santos-Cortes, L. del C., Tejeda-del-Cueto, M.E., 2024. Numerical Analysis and Validation of an Optimized B-Series Marine Propeller Based on NSGA-II Constrained by Cavitation. *Journal of Marine Science and Engineering*, 12(2), 205. <https://doi.org/10.3390/jmse12020205>
- [19] Lu, D., Wang, A., Gan, H., Su, Y., Ao, X., 2025. A multi-objective collaborative optimization method of ship energy efficiency based on NSGA-II and TOPSIS. *Brodogradnja*, 76(3), 76301. <https://doi.org/10.21278/brod76301>
- [20] Vesting, F., Bensow, R.E., 2018. Particle swarm optimization: an alternative in marine propeller optimization? *Engineering Optimization*, 50, 70-88. <https://doi.org/10.1080/0305215X.2017.1302438>
- [21] Ouyang, W., Zhang, Z., Nie, Y., Liu, B., Vanierschot, M., 2025. Parametric modeling and collaborative optimization of a rim-driven thruster considering propeller-duct interactions. *Ocean Engineering*, 337, 121746. <https://doi.org/10.1016/j.oceaneng.2025.121746>
- [22] Zuo, H., Zhao, Y. and Jia, J., 2025. Bayesian-optimized BP neural network for marine propeller design optimization with improved NSGA-III. *Ocean Engineering*, 340, 122375. <https://doi.org/10.1016/j.oceaneng.2025.122375>
- [23] Li, L., Chen, Y., Xie, S., Xiao, Y., Fang, T., Wang, C., 2025. Comprehensive feature-based machine learning for fast prediction of marine propeller's open-water performance. *Applied Ocean Research*, 154, 104310. <https://doi.org/10.1016/j.apor.2024.104310>
- [24] Mathworks, 2025. MATLAB Help Center.

- [25] Auf'm Keller, W. H., 1973. Extended diagrams for determining the resistance and required power for single-screw ships. *International Shipbuilding Progress*, 20, 133-142. <https://doi.org/10.3233/ISP-1973-2022501>
- [26] Tadros, M., Ventura, M., Guedes Soares, C., 2023. Optimization procedures for a twin controllable pitch propeller of a ROPAX ship at minimum fuel consumption. *Journal of Marine Engineering & Technology*, 22, 167-175. <https://doi.org/10.1080/20464177.2022.2106623>
- [27] Larsson, L., Stern, F., Bertram, V., 2003. Benchmarking of Computational Fluid Dynamics for Ship Flows: The Gothenburg 2000 Workshop. *Journal of Ship Research*, 47, 63-81. <https://doi.org/10.5957/jsr.2003.47.1.63>
- [28] Farkas, A., Soonseok, S., Degiuli, N., Martić, I., Demirel, Y. K., 2020. Impact of biofilm on the ship propulsion characteristics and the speed reduction. *Ocean Engineering*, 199, 107033. <https://doi.org/10.1016/j.oceaneng.2020.107033>
- [29] Holtrop, J., Mennen, G. G. J., 1978. A statistical power prediction method. *International Shipbuilding Progress*, 25, 253-256. <https://doi.org/10.3233/ISP-1978-2529001>
- [30] NMRI, 2015. Tokyo 2015 A Workshop on CFD in Ship Hydrodynamics. <https://t2015.nmri.go.jp/index.html> (Accessed 26 February 2026)
- [31] Brodarski Institute, 2022a. Report 6652-M. Resistance, self-propulsion and 3D wake measurement test results, *Brodarski Institute*. Zagreb.
- [32] Degiuli, N., Martić, I., Farkas, A., Pedišić Buča, M., Dejhalla, R., Grlj, C.G., 2023. Experimental assessment of the hydrodynamic characteristics of a bulk carrier in off-design conditions. *Ocean Engineering*, 280, 114936. <https://doi.org/10.1016/j.oceaneng.2023.114936>
- [33] Grlj, C.G., Degiuli, N., Martić, I., 2025a. Assessment of the effect of speed and scale on the total resistance and its components for a bulk carrier. *Results in Engineering*, 26, 105095. <https://doi.org/10.1016/j.rineng.2025.105095>
- [34] Grlj, C.G., Degiuli, N., Martić, I., 2025b. Scale effects on the resistance and propulsion characteristics of the Japan Bulk Carrier. *Ocean Engineering*, 339, 122059. <https://doi.org/10.1016/j.oceaneng.2025.122059>
- [35] Kim, Y., Kim, J.-H., 2016. Benchmark study on motions and loads of a 6750-TEU containership. *Ocean Engineering*, 119, 262-273. <https://doi.org/10.1016/j.oceaneng.2016.04.015>
- [36] Brodarski Institute, 2022b. Report 6655-M. Resistance, self-propulsion and 3D wake measurement test results, *Brodarski Institute*. Zagreb.
- [37] Degiuli, N., Martić, I., Pedišić Buča, M., Grlj, C.G., 2025b. Benchmark study on resistance and propulsion characteristics of a 6750-TEU container ship. *Ocean Engineering*, 319, 120300. <https://doi.org/10.1016/j.oceaneng.2025.120300>
- [38] Grlj, C.G., Degiuli, N., Martić, I., 2023a. The Impact of Numerical Parameters on the Resistance Characteristics of a Container Ship at the Model and Full Scale. *Journal of Marine Science and Engineering*, 11(9), 1672. <https://doi.org/10.3390/jmse11091672>
- [39] Moctar, O.E., Shigunov, V., Zorn, T., 2012. Duisburg Test Case: Post-Panamax Container Ship for Benchmarking. *Ship Technology Research*, 59, 50-64. <https://doi.org/10.1179/str.2012.59.3.004>
- [40] Farkas, A., Degiuli, N., Martić, I., Mikulić, A., 2023. Benefits of slow steaming in realistic sailing conditions along different sailing routes. *Ocean Engineering*, 275, 114143. <https://doi.org/10.1016/j.oceaneng.2023.114143>
- [41] Martić, I., Degiuli, N., Majetić, D., Farkas, A., 2021. Artificial Neural Network Model for the Evaluation of Added Resistance of Container Ships in Head Waves. *Journal of Marine Science and Engineering*, 9(8), 826. <https://doi.org/10.3390/jmse9080826>